ELSEVIER

Journal of Power Sources 104 (2002) 265–271

JOURNAL OF POWER SOURCES

www.elsevier.com/locate/jpowsour

# Effects of $NH_3$ and $NO_x$ on the performance of MCFCs

Makoto Kawase[a,*], Yoshihiro Mugikura[a], Takao Watanabe[a], Yuki Hiraga[b], Toshihide Ujihara[b]

[a]*Central Research Institute of Electric Power Industry, 2-6-1 Nagasaka, Yokosuka, Kanagawa 240-0196, Japan*
[b]*Shikoku Research Institute Incorporated, 2109-8 Yashima-nishimachi, Takamatsu, Kagawa 761-0192, Japan*

Received 16 July 2001; received in revised form 19 September 2001; accepted 25 September 2001

**Abstract**

To evaluate the effect $NH_3$ and $NO_x$ have on the performance of molten carbonate fuel cells (MCFCs), bench-scale cell tests and half-cell experiments have been performed with fuel gas containing $NH_3$, or with oxidant gases containing $NO_x$. Most of the added $NH_3$ is discharged from the anode, and does not affect the cell voltage. The $NO_x$ does harm to the cell voltage during earlier operating stages, but the harm tends to decrease with increasing operating time. The main cause for the cell voltage drop is the increase of internal resistance. As a result of the analyses regarding the electrolyte composition in the operated cells, the gas composition and the cyclic voltammograms, the behavior of $NO_x$ in the cell is found to be as follows: $NO_x$ reacts with the carbonate and dissolves in the electrolyte to make $NO_2^-$ and $NO_3^-$. These ions react with the hydrogen in the fuel gas and lead to the production of $N_2$ and a small amount of $NH_3$. Consequently, $NO_2^-$ and $NO_3^-$ are not accumulated in the electrolyte, and the effect of $NO_x$ on the cell life expectancy is slight. 

*Keywords:* Coal gas; $CO_2$ recycling system; MCFC; $NH_3$; $NO_x$

## 1. Introduction

Coal gas, which is expected to serve as the primary fuel for MCFCs, contains many contaminants such as $H_2S$, HCl, HF and $NH_3$. $NH_3$ is one of these contaminants. The amount of $NH_3$ produced is influenced by the ingredients of coal and the gasification process employed. Generally, the MCFC power plant is equipped with a $CO_2$ recycling system, which completely converts the CO discharged from the anode as $CO_2$ during a catalytic burning process and supplies the cathode with $CO_2$ [1]. $NO_x$ is also generated from $NH_3$ during the catalytic burning process and is used to supply the cathode. Fig. 1 shows the diagram of the gas cycle in MCFCs. For example, if the concentration of $NH_3$ in the anode outlet gas is approximately 250 ppm, the concentration of $NO_x$ in the oxidant gas is calculated to be approximately 20–50 ppm. Therefore, it is necessary to clarify the acceptable $NO_x$ concentration and determine the acceptable $NH_3$ concentration in each power generation system. In this study, we have discussed the effect $NH_3$ and $NO_x$ have on the performance of MCFCs and the behavior of $NO_x$ in half-cell experiments and bench-scale cell tests with the oxidant gas containing different levels of $NO_x$.

## 2. Experiments

### 2.1. Bench-scale cell tests

Cell performance data has been obtained by using bench-scale cells with a 110 $cm^2$ effective electrode area manufactured by Ishikawajima-Harima Heavy Industries Co., Ltd. The cathodes are made of lithiated NiO, and the matrices, which are made of $LiAlO_2$, support a mixture of lithium carbonate and potassium carbonate (Li/K = 70/30 mol% (m/o)), which is used as the electrolyte. The anodes are Ni-based alloys. The basic operating conditions are: temperature 923 K, pressure 2.94 atm and current density 150 mA $cm^{-2}$. For the test, during which $NH_3$ is added to the fuel, gas cylinders containing $H_2$ and $NH_3$ (3000 ppm) are prepared, and the flow rates of the main gas ($H_2/CO_2/H_2O$) and sub-gas ($H_2/NH_3$) are regulated for a target concentration of $NH_3$. Whereas for the test, during which $NO_x$ is added to the oxidant gas, we prepared gas cylinders containing $N_2$ and NO (900 ppm). The flow rates of the main gas ($N_2/CO_2/O_2$) and sub-gas ($N_2$/NO) are regulated for a

* Corresponding author.
*E-mail address*: kawase@criepi.denken.or.jp (M. Kawase).

0378-7753/02/$ – see front matter 
PII: S0378-7753(01)00949-1

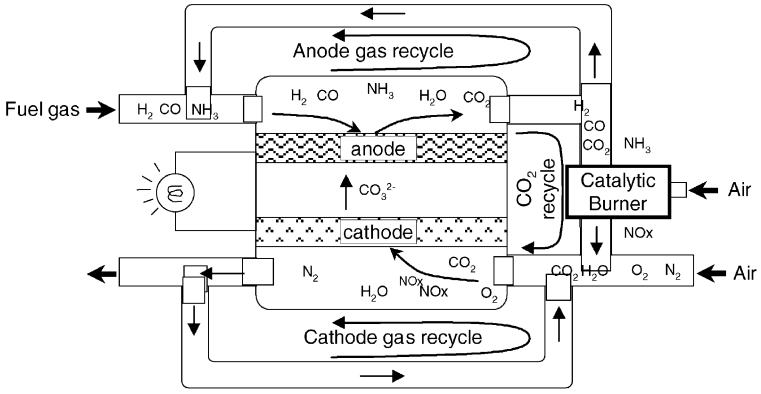


Fig. 1. Diagram of gas cycle in MCFC.

target concentration of $NO_x$. A part of the added NO reacts with the $O_2$ to form $NO_2$. The concentration of $NO_x$ in the inlet and outlet gases is analyzed by using gas analyzers manufactured by Horiba Co., Ltd.

In general, the performance of a MCFC can be expressed by the following equation:

$$V = E - \eta_{ne} - (R_{ir} + R_{re}) \times J \quad (1)$$

where $V$ (V) is the actual cell voltage, $E$ (V) the equilibrium voltage (open-circuit voltage), $\eta_{ne}$ (V) the Nernst loss, $R_{ir}$ ($\Omega\ cm^2$) is the internal resistance, $R_{re}$ ($\Omega\ cm^2$) the reaction resistance, and $J$ (A $cm^{-2}$) is the current density. The actual cell voltage, the equilibrium voltage and the internal resistance are measured, whereas, the Nernst loss and the reaction resistance are estimated by using the Morita equation [2].

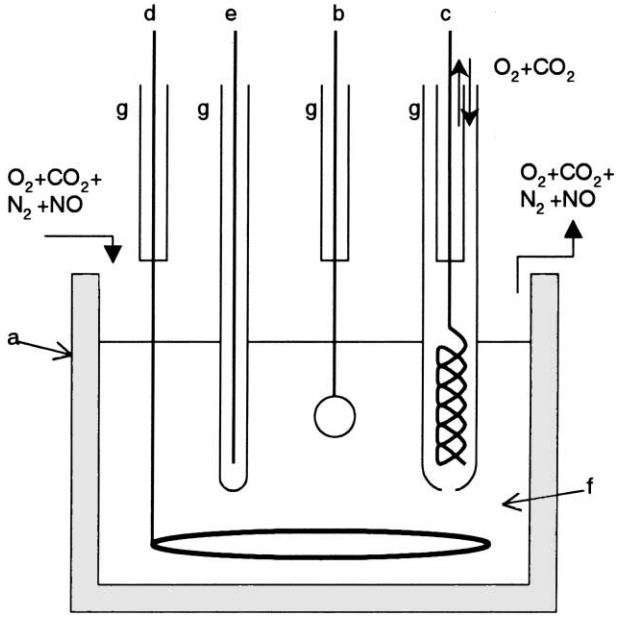


Fig. 2. Schematic diagram of experimental cell: (a) $Al_2O_3$ crucible; (b) working electrode; (c) reference electrode; (d) counter electrode; (e) thermocouple; (f) electrolyte; (g) $Al_2O_3$ tube.

### 2.2. Cyclic voltammetry

To investigate the state of the nitrogen oxides in the electrolyte, half-cell experiments are performed. Fig. 2 shows the schematic diagram of the experimental cell. The chamber containing the cell is especially designed for controlling the atmosphere. The working electrode is a gold plate (Ø 5 mm, $t = 0.1$ mm), the counter electrode a gold-ringed wire. The potentials refer to a Au ($O_2$/$CO_2$ = 33/67%) reference electrode. A mixture of lithium carbonate and potassium carbonate (Li/K = 62/38 mol% (m/o)) is used as the electrolyte. The supplied gases are mixtures of $N_2$, $CO_2$ and $O_2$. For the test with $NO_x$, gas cylinders containing $N_2$ and NO (900 ppm) are prepared, and the flow rates of the main gas ($N_2/CO_2/O_2$) and sub-gas ($N_2$/NO) are regulated for a target concentration of $NO_x$.

## 3. Results and discussions

### 3.1. Effect of $NH_3$ on the cell performance

Fig. 3 shows the changes in cell voltage, IR-free voltage and internal resistance by using a single cell operated at 150 mA $cm^{-2}$ and 923 K with $NH_3$ (500 ppm) contained within the fuel gas. The period during which $NH_3$ is added is between 351 and 1531 h. The following has been determined: the cell voltage does not change due to the addition of $NH_3$. As a result of the anode gas analysis, the concentration of $NH_3$ in the outlet gas is almost equal to that in the inlet gas from early stages of the addition. Therefore, we can establish that $NH_3$ hardly dissolves in the electrolyte and does not react with the carbonate. Hence, approximately 500 ppm $NH_3$ is harmless to the cell performance.

### 3.2. Effect of $NO_x$ on the cell performance

Fig. 4 shows the changes in cell voltage, IR-free voltage and internal resistance in a single cell operated at 150 mA $cm^{-2}$ and 923 K with $NO_x$ (50 ppm) contained in the oxidant gas. $NO_x$ is added during two periods, namely

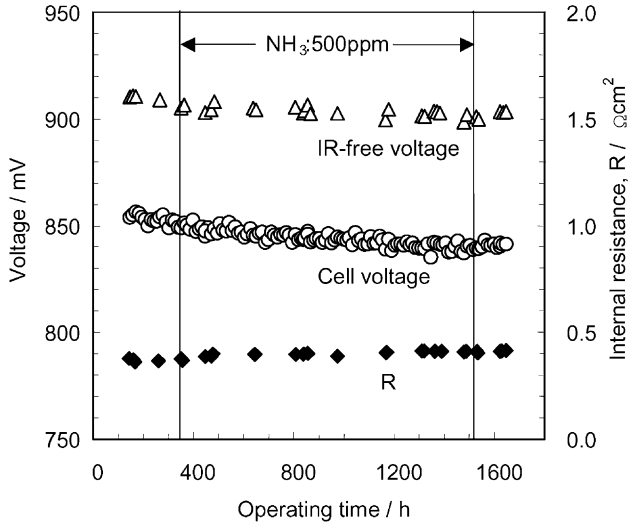


Fig. 3. Changes of cell voltage, IR-free voltage and internal resistance in a single cell operated at 150 mA $cm^{-2}$ and 923 K with $NH_3$ impurity in the oxidant gas. Oxidant gas composition: $N_2/O_2/CO_2 = 55/15/30$; $U_{ox}$, 40%. Fuel gas composition: $H_2/CO_2/H_2O = 64/16/20$; fuel utilization, 60%; pressure, 2.94 atm.

between 500 and 1462 h and between 1849 and 4173 h. The total time of added $NO_x$ results to 3300 h. It has been found that the cell performance drops due to the $NO_x$ addition. During both periods, the cell voltage degradation rate is greater during the early stages, but shows a tendency to decrease with increasing operating time. Between the first and the second period, the internal resistance reduces with operating time, and the cell performance recovers. Since the changes in the IR-free voltage are very small during operation, the increase in internal resistance is responsible for the cell voltage loss. The increase in internal resistance is believed to be due to the low conductive product, which

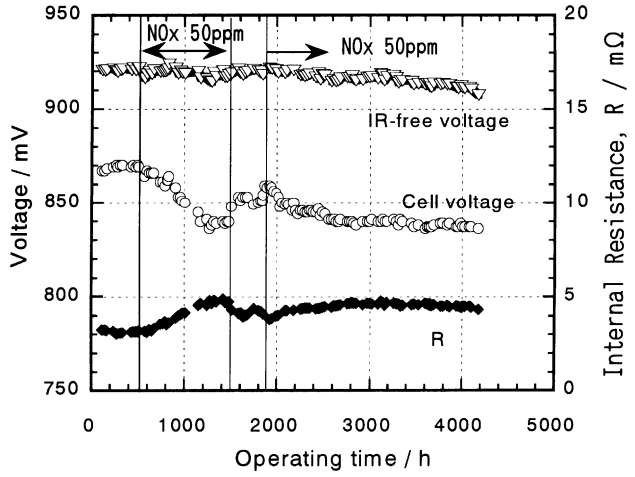


Fig. 4. Changes of cell voltage, IR-free voltage and internal resistance in a single cell operated at 150 mA $cm^{-2}$ and 923 K with $NO_x$ impurity in the oxidant gas. Oxidant gas composition: $N_2/O_2/CO_2 = 55/15/30$; $U_{ox}$, 40%. Fuel gas composition: $H_2/CO_2/H_2O = 64/16/20$; fuel utilization, 60%; pressure, 2.94 atm.

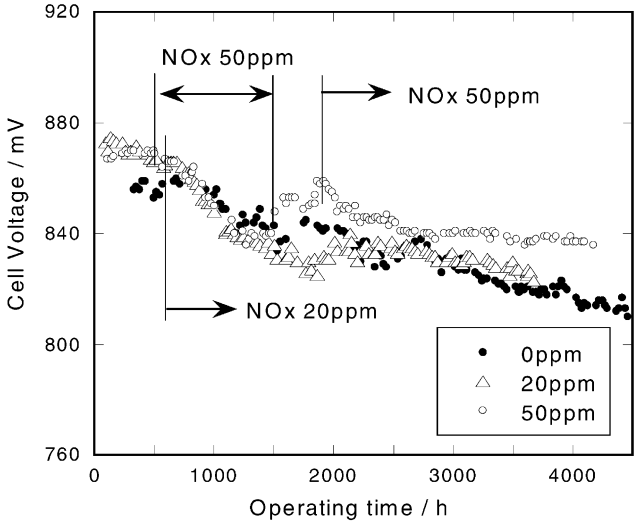


Fig. 5. Cell voltage changes according to various $NO_x$ levels at 150 mA $cm^{-2}$. The operating conditions correspond with Fig. 4.

is created in the reaction of $NO_x$ and the cell components. This low conductive product has a certain saturation point and disintegrates in clean gas conditions. Because nitrate and nitrite ions, which dissolve in the electrolyte, have a higher conductivity than carbonate ions, the product can be found in the corrosion layer in the current collector.

Moreover, in the test with 20 ppm $NO_x$, the main cause for the cell voltage loss is also the increase in internal resistance. Fig. 5 shows the cell voltage changes with 20 and 50 ppm $NO_x$ and without $NO_x$. The cell voltage degradation rate is larger in the early adding stages, but the increase rate of the internal resistance diminishes with increasing operating time. Furthermore, the cell performance with 20 ppm $NO_x$ is almost equal to that without $NO_x$ after 2000 h.

### 3.3. Behavior of nitride compounds in the cell

To explain the pattern of the cell voltage decline, we would like to discuss the state of nitride compounds in the electrolyte, the removal ratio of $NO_x$ and the behavior of nitride compounds in the cell.

### 3.4. State of nitride compounds in the electrolyte

It has been reported that $NO_2$ is absorbed by molten alkali carbonate to form nitrites and nitrates according to the following reaction [3]:

$$M_2CO_3 + 2NO_2 \rightarrow MNO_2 + MNO_3 + CO_2 \quad (2)$$

where M is the alkali metal.

The relation between $NO_2^-$ and $NO_3^-$ in correspondence with the molten alkali nitrate and nitrite has been discussed by many scientists [4–9]. Nitrite is formed by the thermal decomposition equilibrium [4,5]:

$$NO_3^- \leftrightarrow NO_2^- + \tfrac{1}{2}O_2 \quad (3)$$

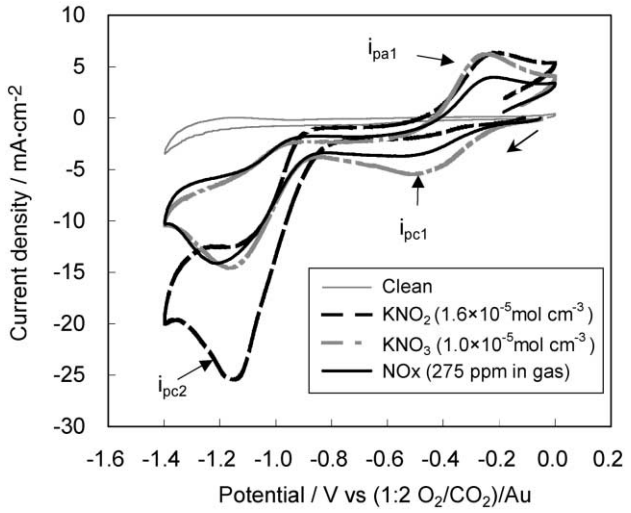


Fig. 6. Cyclic voltammograms for Au electrode in $Li_2CO_3$–$K_2CO_3$ eutectic melt at 923 K, scan rate 0.2 V $s^{-1}$. The gas composition is 55% nitrogen, 15% oxygen and 30% carbon dioxide.

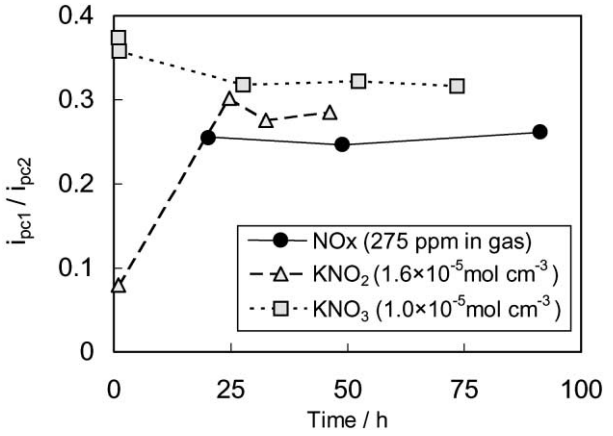


Fig. 7. Change in ratio of two peak current ($i_{pc1}/i_{pc2}$) with time after an addition of $NO_x$ (275 ppm in the gas as in Fig. 6), $KNO_2$ ($1.6 \times 10^{-5}$ mol $cm^{-3}$ in the electrolyte), or $KNO_3$ ($1.0 \times 10^{-5}$ mol $cm^{-3}$ in the electrolyte).

Furthermore, the relation between $NO_3^-$ and $NO_2^-$ depends on the super oxide and power oxide ions, which are formed during the following reactions [6–8]:

$$NO_3^- + O^{2-} \leftrightarrow NO_2^- + O_2^{2-} \quad (4)$$

$$2NO_3^- + O_2^{2-} \leftrightarrow 2NO_2^- + 2O_2^- \quad (5)$$

Similarly, the same reactions can be seen regarding the molten alkali carbonate.

The state of nitrogen oxides in the electrolyte has been investigated by applying the cyclic voltammogrammetry. Fig. 6 presents the cyclic voltammograms after the addition of $NO_x$ (275 ppm into the gas), $KNO_2$ ($1.6 \times 10^{-5}$ mol $cm^{-3}$ into the electrolyte), and $KNO_3$ ($1.0 \times 10^{-5}$ mol $cm^{-3}$ into the electrolyte). The cyclic voltammograms of the $KNO_2$ and $KNO_3$ additions are measured 1 h after the addition, whereas the cyclic voltammogram of $NO_x$ is measured 91 h after adding $NO_x$. Two cathodic peaks ($i_{pc1}$, $i_{pc2}$) and one anodic peak ($i_{pa1}$) are observed at −0.4, −1.2 and −0.2 V in all voltammograms. The peak currents depend on the additives and change with time. Fig. 7 shows the change in peak current ratios ($i_{pc1}/i_{pc2}$) according to time after the addition of $NO_x$, $KNO_2$ and $KNO_3$. Regarding the addition of $KNO_2$ and $KNO_3$, the peak current ratio ($i_{pc1}/i_{pc2}$) moves close to 0.3 with increasing time. On the other hand, regarding the addition of $NO_x$, the peak current ratio is stable at approximately 0.26. However, once the addition of $NO_x$ is stopped, the ratio changes towards 0.3.

In summary, one can say that $NO_x$ reacts with the carbonate, and it is therefore, able to dissolve in the electrolyte as $NO_2^-$ and $NO_3^-$. The $i_{pc2}$ is related to the reduction of $NO_2^-$, because $i_{pc2}$ is larger after the addition of $KNO_2$. Moreover, $NO_2^-$ changes into $NO_3^-$ with time.

On the other hand, $i_{pc1}$ is related to the reduction of $NO_3^-$, because $i_{pc1}$ is larger after the addition of $KNO_3$. Furthermore, $NO_3^-$ decomposes to $NO_2^-$ with time according to the reactions (3)–(5). The concentration of $NO_3^-$ and $NO_2^-$ reaches an equilibrium.

The reduction of $NO_3^-$ and $NO_2^-$ in the LiCl–KCl eutectic is reported by Goto et al. [10]:

$$NO_3^- + 2e^- \rightarrow NO_2^- + O^{2-} \quad (6)$$

$$NO_2^- + 2e^- \rightarrow NO^- + O^{2-} \quad (7)$$

It is known that the concentrations of $O^{2-}$, $O_2^-$ and $O_2^{2-}$ in the Li/K carbonate are higher than those in the LiCl–KCl eutectic. Therefore, the reduction of $NO_3^-$ and $NO_2^-$ in the Li/K carbonate is not only related to $O^{2-}$, but also to $O_2^-$ and $O_2^{2-}$ according to the following reactions:

$$2NO_3^- + e^- \rightarrow 2NO_2^- + O_2^- \quad (8)$$

$$NO_3^- + e^- \rightarrow NO_2^- + \tfrac{1}{2}O_2^{2-} \quad (9)$$

$$2NO_2^- + e^- \rightarrow 2NO^- + O_2^- \quad (10)$$

$$NO_2^- + e^- \rightarrow NO^- + \tfrac{1}{2}O_2^{2-} \quad (11)$$

### 3.5. Behavior of $NO_x$ in MCFCs

We have analyzed the anode and cathode outlet gases in the test shown in Fig. 4. The concentration of $NO_x$ in the cathode outlet gas is stable at approximately 35% of the added $NO_x$. A small amount of $NH_3$, which is approximately 1–3% of the added $NO_x$, is detected. However, other nitrogen compounds, which would be $N_2O$, NO or $NO_2$, are not detected. The content of nitrogen compounds in the electrolyte, which is measured in all cells after completing the tests, is only 0.1–0.3% of the added $NO_x$. Furthermore, we can confirm that $NO_3^-$ and $NO_2^-$ does not decompose immediately during the cooling process in the half-cell experiment. Therefore, nitrogen compounds do not accumulate in the electrolyte.

Table 1
Balance of nitrogen compounds in a single cell operated according to conditions in Fig. 4 and a simulated cell[a]

| | Single cell (%) | Simulated cell (%) |
|---|---|---|
| $NO_x$ at the inlet | 100 | 100 |
| $NO_x$ at the outlet (cathode for the single cell) | 32 | 92 |
| $NH_3$ in anode exhaust | 1 | – |
| $NO_2^-$ and $NO_3^-$ accumulated in electrolyte | 0.2 | 8 |
| Not detected | 67 | – |

[a] The simulated cell consists of the same electrolyte plate (carbonated + $LiAlO_2$, without electrodes) as in the single cell, and it is exposed to a gas mixture ($N_2/O_2/CO_2 = 55/15/30$, $NO_x = 50$ ppm, 1027 ml $min^{-1}$).

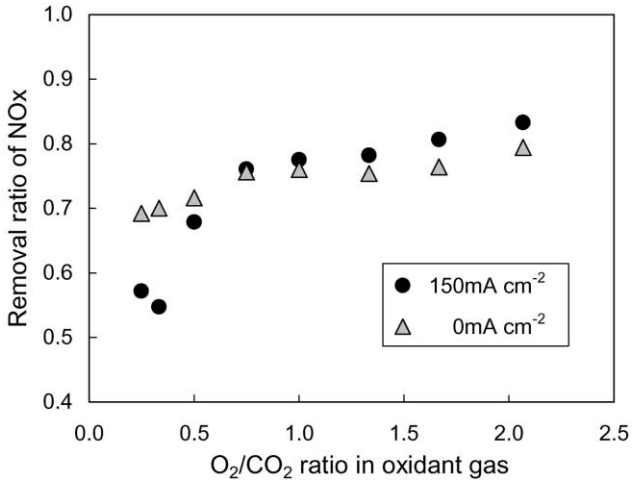


Fig. 8. Effect of oxidant gas composition on removal ratio of $NO_x$. Oxidant gas flow rate, 1046 ml $min^{-1}$; concentration of $NO_x$, 50 ppm. Fuel gas composition: $H_2/CO_2/H_2O = 64/16/20$; fuel utilization at 150 mA $cm^{-2}$, 60%; temperature, 923 K; pressure, 2.94 atm.

To confirm the effect the anode has on the mass balance of nitrogen compounds, we have investigated the solubility of $NO_x$ in the molten carbonate under cathode gas conditions by using a simulated cell. The simulated cell consists of the same electrolyte plate (carbonated + $LiAlO_2$, without electrodes) as the single cell, and it is exposed to the gas mixture $N_2/O_2/CO_2 = 55/15/30$ and $NO_x = 50$ ppm. The flow rate of the oxidant gas is equivalent to that in the single cell test shown in Fig. 4. The gas analysis shows that the amount of $NO_x$ in the outlet gas is approximately 92% of the added $NO_x$ 2 h after the addition. Hence, only 8% of the added $NO_x$ is absorbed by the carbonate. This result is different from that of the single cell test, as listed in Table 1. North American Rockwell Co. has reported that the absorption ratio of $NO_x$ in alkali carbonates is over 50% in gas conditions without $CO_2$, but that the absorption rate is under 15% in gas conditions with $CO_2$ [11]. This result corresponds with the result of the simulated cell test. Therefore, the continuous and high removal ratio of $NO_x$ in the single cell depends on the anode. The general belief is that $NO_2^-$ and $NO_3^-$ are not accumulated in the electrolyte and that they change into nitrogen at the anode where they are continuously exhausted.

### 3.6. Removal ratio of $NO_x$

#### 3.6.1. Effects of oxidant gas composition

While the experimental conditions of the fuel gas and the flow rate of the oxidant gas are stable, the concentration of $NO_x$ in the cathode outlet gas is measured at various oxidant gas compositions. Fig. 8 presents the effect the oxidant gas composition has on the $NO_x$ removal ratio. The removal ratio of $NO_x$ is defined as

$$\text{removal ratio of } NO_x = 1 - \frac{\text{flow rate of oxidant outlet gas} \times NO_x \text{ concentration in oxidant outlet gas}}{\text{flow rate of oxidant inlet gas} \times NO_x \text{ concentration in oxidant inlet gas}} \quad (12)$$

We have been able to determine an improvement in the $NO_x$ removal ratio at a higher $O_2/CO_2$ ratio. This dependence of the $O_2/CO_2$ ratio proves that the dissolution of $NO_x$ in the electrolyte is related to the following reactions:

$$2NO + \tfrac{3}{2}O_2 + M_2CO_3 \rightarrow 2MNO_3 + CO_2 \quad (M = Li, K) \quad (13)$$

$$2NO + \tfrac{1}{2}O_2 + M_2CO_3 \rightarrow 2MNO_2 + CO_2 \quad (M = Li, K) \quad (14)$$

$$2NO_2 + \tfrac{1}{2}O_2 + M_2CO_3 \rightarrow 2MNO_3 + CO_2 \quad (M = Li, K) \quad (15)$$

#### 3.6.2. Effects of the fuel gas composition

While the experimental conditions of the oxidant gas are stable, the concentration of $NO_x$ in the cathode outlet gas is measured at various fuel gas compositions. Fig. 9 shows the effect the fuel gas composition has on the $NO_x$ removal ratio. We have been able to detect an improvement in the $NO_x$ removal ratio at a higher $H_2$ concentration. As mentioned above, a small amount of $NH_3$ is contained in the anode outlet gas, whereas, other nitrogen compounds are not contained in the mentioned gas. Therefore, it is assumed that most of the $NO_2^-$ and $NO_3^-$ reacts with the $H_2$ to form $N_2$ according to the following reactions:

$$2NO_3^- + 6H_2 \rightarrow N_2 + 6H_2O + 2e^- \quad (16)$$

$$2NO_2^- + 4H_2 \rightarrow N_2 + 4H_2O + 2e^- \quad (17)$$

$$2NO_3^- + 5H_2 \rightarrow N_2 + 4H_2O + 2OH^- \quad (18)$$

$$2NO_2^- + 3H_2 \rightarrow N_2 + 2H_2O + 2OH^- \quad (19)$$

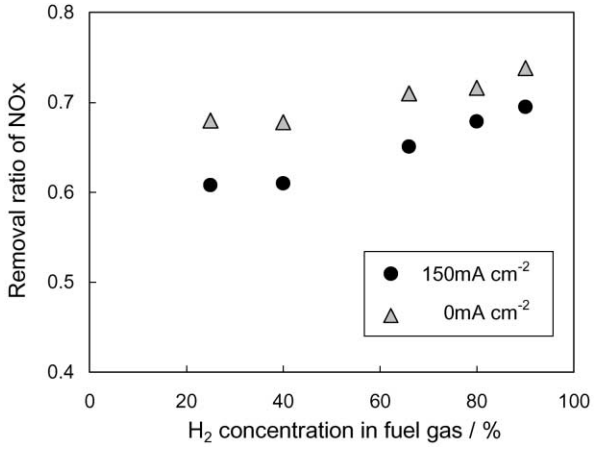


Fig. 9. Effect of $H_2$ concentration in fuel gas on removal ratio of $NO_x$. Oxidant gas composition: $N_2/O_2/CO_2 = 55/15/30$; concentration of $NO_x$, 50 ppm; fuel utilization at 150 mA $cm^{-2}$, 60%; temperature, 923 K; pressure, 2.94 atm.

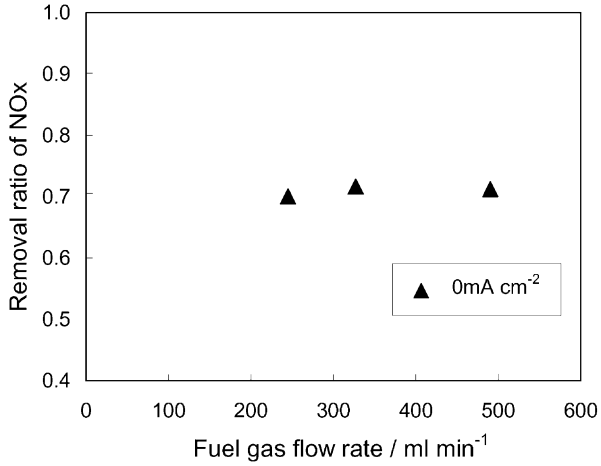


Fig. 11. Effect of fuel gas flow rate on removal ratio of $NO_x$. Oxidant gas composition: $N_2/O_2/CO_2 = 55/15/30$; concentration of $NO_x$, 50 ppm; oxidant gas flow rate, 1046 ml $min^{-1}$. Fuel gas composition: $H_2/CO_2/H_2O = 64/16/20$; temperature, 923 K; pressure, 2.94 atm.

### 3.6.3. Effects of the fuel and oxidant gas flow rate

Fig. 10 shows the effect the oxidant gas flow rate has on the removal ratio of $NO_x$. The amount of $NO_x$ and NO in the cathode outlet gas is proportional to the amount of added $NO_x$. The following relations express this phenomenon.

$$\text{Exhausted NO}_x = 0.60 \times (\text{added NO}_x) - 2.3 \times 10^{-7} \quad (\text{mol min}^{-1})$$

$$\text{Exhausted NO} = 0.36 \times (\text{added NO}_x) - 1.3 \times 10^{-7} \quad (\text{mol min}^{-1})$$

The removal ratio of $NO_x$ moves close to 40% as the oxidant gas flow rate increases. Therefore, the dissolution of $NO_x$ in the electrolyte corresponds with Henry's law.

Fig. 11 expresses the effect the fuel gas flow rate has on the removal ratio of $NO_x$, which is independent of the fuel gas flow rate. Hence, some of the reactions, which refer to the reactions (16)–(19), take place very quickly.

### 3.6.4. Effect of the current density

Fig. 12 presents the effect the current density has on the removal ratio of $NO_x$. If we consider the change of the cathode outlet gas flow rate and the gas composition according to the current density, the effect of the current density is negligible compared to the effect other factors have on the removal ratio. Therefore, it is almost definite that $NO_2^-$ or $NO_3^-$ react with $H_2$ according to the reactions (18) and (19).

We have come to a conclusion regarding the behavior of $NO_x$ in the cell, which can be seen in Fig. 13. First of all, at the cathode, $NO_x$ reacts with the carbonate and dissolves into

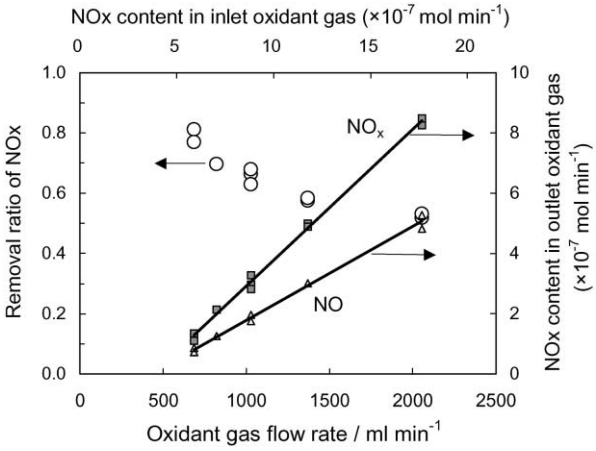


Fig. 10. Effect of oxidant gas flow rate on removal ratio of $NO_x$. Oxidant gas composition: $N_2/O_2/CO_2 = 55/15/30$; concentration of $NO_x$, 20 ppm. Fuel gas composition: $H_2/CO_2/H_2O = 64/16/20$; fuel gas flow rate, 327 ml $min^{-1}$; current density, 150 mA $cm^{-2}$; fuel utilization, 60%; temperature, 923 K; pressure, 2.94 atm.

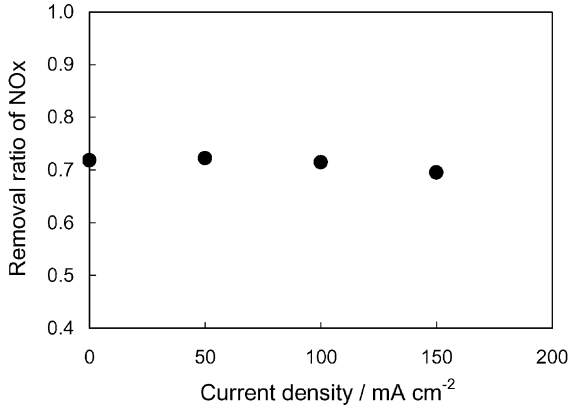


Fig. 12. Effect of current density on removal ratio of $NO_x$. Oxidant gas composition: $N_2/O_2/CO_2 = 55/15/30$; concentration of $NO_x$, 20 ppm. Fuel gas composition: $H_2/CO_2/H_2O = 64/16/20$; oxidant gas flow rate, 1046 ml $min^{-1}$; fuel gas flow rate, 327 ml $min^{-1}$; temperature, 923 K; pressure, 2.94 atm.

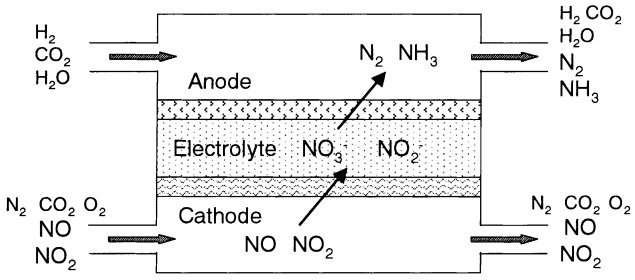


Fig. 13. Behavior of $NO_x$ in MCFC.

$NO_2^-$ and $NO_3^-$ in the electrolyte. Secondly, at the anode, $NO_2^-$ and $NO_3^-$ react with $H_2$ and change into $N_2$ and a small amount of $NH_3$. Finally, $N_2$ and $NH_3$ are discharged from the anode outlet so that nitrogen compounds do not accumulate in the cell. The generation of substances, which cause the increase in internal resistance, is slow, and the cell performance does not drop by adding $NO_x$. Furthermore, this result shows that $NO_x$ is purified and changed into $N_2$, and that structures like MCFCs have the function of removing $NO_x$ from the oxidant gas.

## 4. Conclusions

1. $NH_3$ does not lessen the performance of the MCFCs, and most of the added $NH_3$ is discharged from the anode outlet.
2. In bench-scale cell tests, the addition of $NO_x$ triggers a step by step increase of internal resistance, which causes the cell voltage to drop. However, this effect tends to decrease with increasing operating time. Because the cell voltage recovers during an interruption of adding $NO_x$, the cause of the increase in internal resistance is the production of low conductive substances, which disintegrate in clean gas conditions.
3. $NO_x$ reacts with the carbonate at the cathode and dissolves into $NO_2^-$ and $NO_3^-$ in the electrolyte. $NO_2^-$ and $NO_3^-$ react with $H_2$ and change into $N_2$ and small amounts of $NH_3$ at the anode. Finally, $N_2$ and $NH_3$ are discharged from the anode outlet. Therefore, nitrogen compounds do not accumulate in the cell, and the high removal ratio of $NO_x$ is maintained. Moreover, the generation of the substances, which cause the increase in internal resistance, is slow, and consequently the drop of the cell performance by adding $NO_x$ is small.

## Acknowledgements

Part of this work was conducted in cooperation with the New Energy and Industrial Technology Development Organization (NEDO) and the Technology Research Association for Molten Carbonate Fuel Cell Power Generation System (MCFC) in the context of the New Sunshine Program of Ministry of International Trade and Industry (MITI). We appreciate everybody's advice and support.

## References

[1] A.J. Appleby, F.R. Foulkes, Fuel Cell Handbook, 1989, 98 pp.
[2] H. Morita, Y. Mugikura, Y. Izaki, T. Watanabe, T. Abe, J. Electrochem. Soc. 145 (1998) 1511.
[3] W. Bartok, A.R. Crawford, H.J. Hall, E.H. Manny, A. Skopp, Systems Study of Nitrogen Oxide Control Methods for Stationary Sources, Final Report, Vol. 2, NAPCA Contract PH-22-68-55, Report GR-2-NOS-69, 1969.
[4] R.N. Kust, J.D. Burke, Inorg. Nucl. Chem. Lett. 6 (1970) 333.
[5] E.S. Freeman, J. Phys. Chem. 60 (1956) 1487.
[6] P.G. Zambonin, J. Jordan, J. Am. Chem. Soc. 89 (1967) 6365.
[7] P.G. Zambonin, J. Jordan, J. Am. Chem. Soc. 91 (1969) 2225.
[8] P.G. Zambonin, Electroanal. Chem. 45 (1973) 451.
[9] D.H. Kerridge, Molten Salt Forum 5/6 (1998) 469.
[10] T. Goto, M. Tada, T. Ito, Electrochim. Acta 39 (1994) 1107.
[11] Atomics International—North American Rockwell Corp. Monthly Progress Report, 1 December 1968 to 1 January 1969, Contract PH 86-67-128.